Laser-Augmented Micro-Pulsejet Thruster

IEPC-2007-245

Presented at the 30th International Electric Propulsion Conference, Florence, Italy
September 17-20, 2007

Sou Eto[*] and Hideyuki Horisawa[†]
Tokai University, Hiratsuka-shi, Kanagawa, 259-1292, Japan

and

Itsuro Kimura[‡]
Professor Emeritus, University of Tokyo, Bunkyo-ku, Tokyo, 113-8856, Japan

Abstract: A fundamental study of a laser-augmented micro-pulsejet thruster was conducted for a candidate of next-generation air-breathing micro-thruster systems. CFD analyses were conducted to evaluate internal phenomena and thrust performances for propellants of hydrogen-air mixture including effectiveness of an exhaust orifice. Experimental investigations were also conducted to evaluate effectiveness of the orifice and optimum geometries of the micro combustor. From the results, it was shown that the increase of laser energy and reduction of orifice diameter were more effective for thrust-performance improvement. Moreover, it was shown that narrower configuration of the combustor was also effective.

Nomenclature

P_h	=	pressure at the closed edge center [Pa]
P_a	=	atmosphere pressure [Pa]
A	=	cross section of combustion chamber [m^3]
I_{bit}	=	impulse bit [Nsec]
dt	=	time step

1. Introduction

Recent significant development of microelectromechanical systems (MEMS) and precision mechanical machining techniques along with evolution of high-functional materials has enabled various novel micro-electronic devices used in many fields. In aerospace engineering fields, for example, small-sized satellites such as micro- and nano-satellites, and unmanned micro aerial vehicles (MAVs) are under significant development in many countries. Some of the primary elements of these systems are fabricated with those techniques. Specific to controlling aerial vehicles in atmosphere, they are subjected to relatively large aerodynamic forces, and these forces can be used for position and attitude control mechanisms. Utilization of the aerodynamic forces can vary the type of

[*] Graduate Student, Department of Aeronautics and Astronautics, email: 6amjm014@keyaki.cc.u-tokai.ac.jp
[†] Associate Professor, Department of Aeronautics and Astronautics, email: horisawa@keyaki.cc.u-tokai.ac.jp
[‡] Professor Emeritus, University of Tokyo

the mechanisms or configurations of vehicles such as fixed-wings, rotating-wings, or beating-wings, aimed for various purposes.

Authors have been developing of micro air-breathing thrusters, which can be utilized either for primary propulsion engines or attitude control thrusters, or for both purposes. The main objective of this development is to achieve the microthrusters capable of both highspeed transportation and stable hovering. Various small-sized air-breathing propulsion systems such as turbojet and pulsejet engines have been developed for decades and some of them at present are commercially available mostly for hobby-airplane use. Among these systems, authors have been focusing on pulsejets. None of turbo-machinery elements were used in this type of engine, and the propulsion system can be very simple and lightweight. In addition, comparing to other air-breathing systems, its specific impulse and thrust efficiency are relatively high. Although these advantages, noise through the pulse operation is the primary issues.

To achieve the increased initial pressure and namely smaller diameter of the combustor, authors have been trying to use the blast waves induced with focused laser beams. Depending on laser energy, strength of the initial blast wave can be controlled. With this process, initial internal pressure inside the combustor can be abruptly increased.[1]

Since small-sized combustors or micro-PDEs are of our primary concern, ratios of laser energies to heat release from combustion reaction of the combustor can be easily controlled. Therefore, augmented ignition techniques such as laser ignition can be utilized and effective. Along with the miniaturization, area-to-volume ratios of the combustors will increase. With the increased ratios, surface catalytic reactions can be utilized and effective for augmentation of ignition reactions. Moreover, since they are small, the repetitive pulse operation can be in high-repetition rate with proper air-intake mechanisms capable of high-repetition operation. In addition, total force acting on an inner surface of the combustor can be insignificant due to the small surface area. Therefore, strength of the combustor wall can be easily maintained.

In this study, an assessment of thruster performance was conducted by computational fluid dynamic simulations. Our concerns are to elucidate the effects of laser augmentation in the small combustor, combustor configuration and ignition points. Moreover, a fundamental experiment of a laser-augmented micro-pulsejet thruster was also conducted. Thrust performances were tested with a ballistic pendulum type thrust-stand for propellants of hydrogen-air mixtures with various equivalence ratios. Spark-ignition and laser-ignition were also compared to elucidate the optimum ignition schemes and conditions.

2. CFD Simulation of Micro-Pulsejet Thruster

2.1 Simulation Model

We conducted the numerical analysis to verify hydrodynamic and chemical-reaction effects on ignition and subsequent impulse generation phenomena with computational fluid dynamic (CFD) analyses. In the analyses a commercial CFD code, CFD2000 (Adaptive Research Inc.), was utilized. A numerical thruster model consists of a cylindrical combustion chamber (inner diameter of 10 mm x length of 30 mm) having an open orifice and another edge closed. In the analyses, a two-dimensional rectangular geometry is assumed, which consists of an upper half of the chamber from the centerline as shown in Fig.1. A lower side of this model is assumed as a reflective condition and an extra exhaust volume is added after the orifice exit. In the calculation, a time-dependent Navier-Stokes equation including finite rate chemistry of 16-step-elementary reactions of a hydrogen-air mixture is solved.

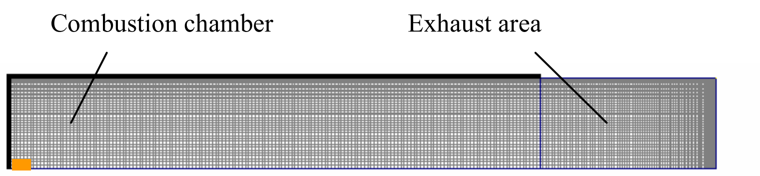

Figure 1. Calculation model.

The sixteen pairs of elementary reactions for 10 species (H_2, O_2, O, H, N, OH, NO, H_2O, HO_2 and N_2) employed in this simulation are listed in Table 1.

As for an initial propellant filling the combustor a hydrogen-air mixture with an ideal mixture of its equivalence ratio of unity was assumed at pressure of 101.3kPa and temperature of 298.15K.

To model a focused laser beam or laser induced plasma, several attempts have been conducted.[2-8] Since a laser pulse is shorter than 10 nsec, its short-duration heating process can be regarded as if occurring under a constant volume condition. For this reason, a high-enthalpy laser-induced plasma kernel is assumed as a hot-gas spot with finite size to which it has developed from an initial micro-plasma nucleus.[8] Since it is confirmed from our experiment that an initial plasma, or hot spot, is as big as 1 ~ 2 mm in diameter at initial 100 nsec, initial size of the spherical hot spot used in this simulation is assumed to be 1 ~ 2 mm in diameter depending on laser pulse energies. Initial pressure and temperature of the hot spot, or laser-induced plasma, were assumed as 1.0 MPa and 3,000 K, respectively. Similar to our experimental conditions, a focal point of the laser beam, or location of the initial plasma, was placed nearby the closed edge on the centerline.

Table 1. 16 elementary reactions with 10 species for hydrogen-air mixture.

1	$H_2 + O_2$	□	$OH + OH$
2	$H_2 + OH$	□	$H_2O + H$
3	$H + O_2$	□	$OH + O$
4	$O + H_2$	□	$OH + H$
5	$H + O_2 + N_2$	□	$HO_2 + N_2$
6	$OH + HO_2$	□	$H_2O + O_2$
7	$H + HO_2$	□	$OH + OH$
8	$O + HO_2$	□	$O_2 + OH$
9	$OH + OH$	□	$O + H_2O$
10	$H_2 + N_2$	□	$H + H + N_2$
11	$O_2 + N_2$	□	$O + O + N_2$
12	$H + OH + N_2$	□	$H_2O + N_2$
13	$O + N_2$	□	$NO + N$
14	$N + O_2$	□	$NO + O$
15	$OH + N$	□	$NO + H$
16	$H + HO_2$	□	$H_2 + O_2$

In our simulation, first of all, an assessment of effects of the orifice diameter on impulse-bits was conducted. The impulse-bit was calculated by integrating temporal changes of local pressures on inner walls of the combustor, as follows,

$$I_{bit} = \int_0^t \int_A (P_h - P_a) dA dt \qquad (1)$$

where p_h: local wall pressure, p_a: ambient (atmospheric) pressure, dA: elemental area at wall, A: total wall area in the simulation domain, t: typical pressure wave duration (1 msec). Secondly, influences of the initial laser-focal points, or laser-induced plasma positions, were investigated. In this simulation, several positions from 0 mm to 30 mm away from the initial focal point at the closed-side of edge were tested as illustrated in Fig.1. Impulse-bits for each case was estimated and then compared.

2.2 Simulation Results and Discussion

Behaviors of pressure wave propagation are shown in Fig.2. It can be seen that the mixture is ignited with a laser-induced plasma and that a pressure wave is running toward the orifice.

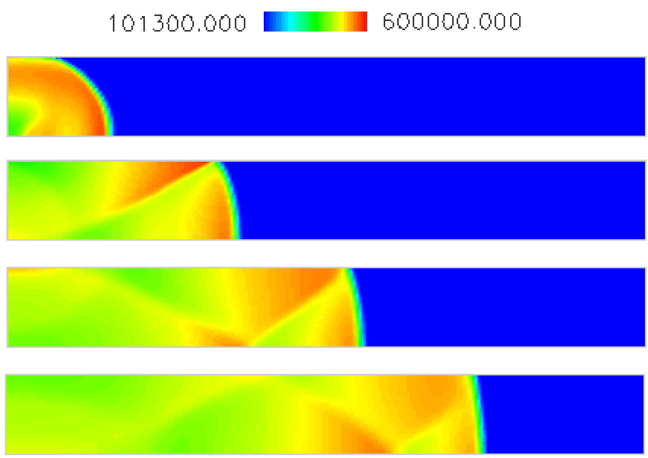

Figure 2. Propagation of pressure wave.

The pressure wave is arriving at the orifice in about 36 μsec after ignition. According to this duration and the distance between the orifice and combustor edge, an average velocity of the pressure-wave propagation is about 833 m/sec. This velocity is faster than the acoustic velocity for the initial flow field.

Temporal variations of internal pressure on centerline at the closed-edge are shown in Fig.3, in which influence of the orifice sizes, between 4 mm and 10 mm in diameters, is compared. With the 10 mm orifice, or without orifice, the internal pressure converges down to ambient pressure at 0.4 msec. Whereas with 4 mm orifice, the advantage in high-pressure becomes significant from 0.1 msec, and it can be maintained for a longer duration which is converging down to ambient pressure at 0.8 msec. The effect of the orifice is remarkable keeping internal pressure higher for longer duration.

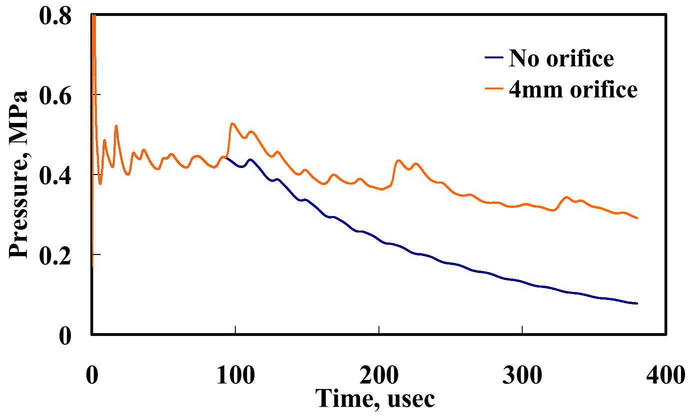

Figure 3. Temporal variations of pressure at closed edge center

The values of impulse-bits calculated from Eq. (1) for above different orifice conditions are listed in Table 2. From the results, the impulse-bit with 4 mm orifice is augmented about 2 times greater than that without orifice. This is due to the higher internal pressure maintained for longer duration.

Results for influences of the laser-focal point on impulse-bit generation are listed in Table 3. Although little difference can be seen among these results, within 1 to 2 %, larger distance of the ignition point away form the closed edge showed slightly greater values of impulse-bits.

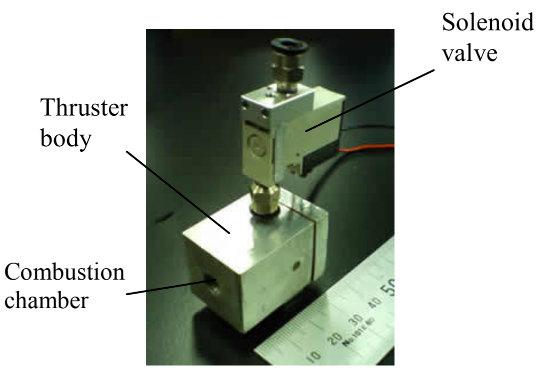

Figure.4 Schematic image of micro thruster

Table 2. Impulse bit (No orifice & Orifice)

	Impulse bit, Nsec/m^2
No orifice	81.6
4mm orifice	150

Table 3. Impulse bit (Ignition point)

distance, mm	Impulse bit, Nsec/m^2
0	79.5
10	83.1
20	83.2
30	83.8

3. Experimental

3.1. Impulse-bit Measurement

A schematic of a thruster is shown in Fig.4. The thruster consists of a cylindrical combustion chamber (inner diameter of 10 mm x length of 30 mm) and an initiator part (inner diameter of 10 mm x length of 5 mm) both made of aluminum.

Schematics of experimental setups showing different ignition methods, a spark ignition and laser ignition, are illustrated in Figs.5 (a) and (b), respectively. In this experiment, a hydrogen-air mixture is used for the propellant. Using solenoid valves, mass flows of hydrogen and air, or equivalence ratios, can be controlled, and introduced into the combustion chamber. In the spark ignition, an electric circuit consisting of a DC charger, a capacitor of 1 μF, and discharge igniter was developed and tested. The capacitor can be charged up to 590 V. As for a miniaturized ignition plug, an in-house plug consisting of a tungsten-rod cathode of 3 mm in diameter and an annular stainless anode of 5 mm in outer-diameter. Changing charge voltages V to the capacitor C, ignition energy E ($E = CV^2/2$) can be controlled. On the other hand, in laser ignition, a laser pulse from an Nd:YAG laser (QUANTEL LPY 150-10/20, wavelength: 1064 nm, maximum pulse energy: 335 mJ/pulse, pulse width: 5 nsec) was irradiated and focused with a focusing lens of f = 150 mm into an initiator part of a cylindrical combustion chamber filled with a hydrogen-air mixture of a controlled equivalence ratio. Then with a laser-induced plasma, a chemical detonation is initiated, and an impulse is generated on the nozzle.

To elucidate influences of ignition method and energy, thrust performance tests were conducted. To measure a single impulse of μNsec-class, a thrust stand was developed and utilized. The thrust stand, shown in Fig.6, consists of a ballistic pendulum. As for its pivot, a knife edge was used. The pendulum is made of an aluminum member of 456 mm in length and 25 mm x 25 mm in cross section. A counter weight was placed in another side of the pendulum to make the pivot as a center of impact. An eddy-current type displacement sensor was used to measure the displacement of the pendulum. A schematic of an experimental setup for impulse-bit measurement is shown in Fig.7. The pendulum receives a reaction force from the thruster and then a displacement or impulse is to be measured. The displacement induced at each impulse generation was calibrated with an impact of an aluminum ball at each shot.

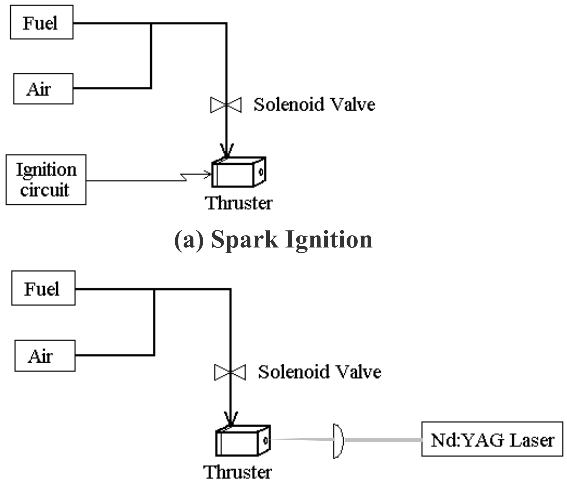

(a) Spark Ignition

(b) LASER Ignition

Figure 5. Schematic of laser ignition systems.

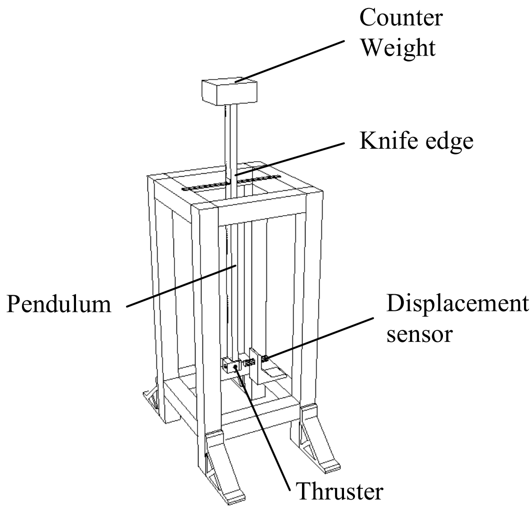

Figure 6. Schematic of impulse

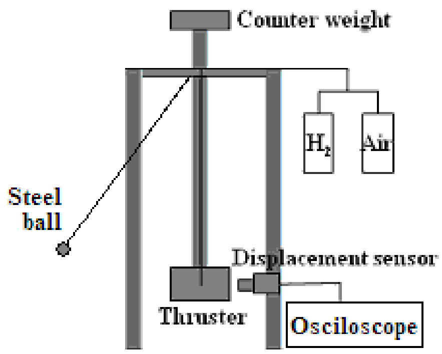

Figure 7. Schematic of calibration setup

3.2. Calibration of Thrust Stand

A schematic of an experimental setup for impulse-bit calibration is also illustrated in Fig.7. The pendulum receives a reaction force from the thruster and then a displacement or impulse is to be measured. The displacement induced at each impulse generation was calibrated with an inelastic impact of an aluminum ball suspended with a string released from an arbitrary height at each measurement, giving an arbitrary impulse to the thruster. A typical output signal of the displacement sensor is shown in Fig.8.

Then relation of an amplitude of the first peak of the signal from the displacement sensor versus an arbitrary impulse is plotted in Fig.9. The impulse was calculated from the height and mass of the impacting ball. As shown in this figure, linear relations between impulse and sensor amplitude can be obtained. From this linear relation, measured values of impulse-bits were estimated.

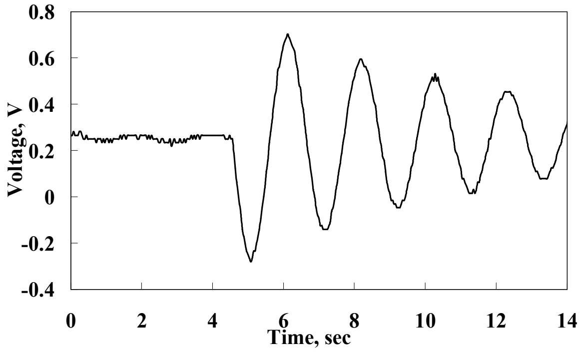

Figure 8. Typical output signal of displacement sensor

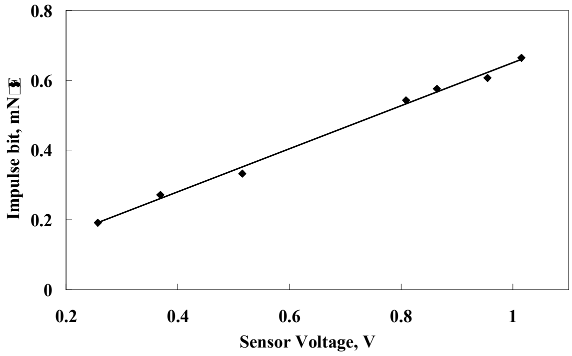

Figure 9. The result of calibration experiment

4. Experimental Results and Discussion

4.1. Comparison of Thrust Performances between Spark Ignition and Laser Ignition

Comparison of thrust performances between conventional spark ignition and laser ignition is shown in Fig.10, in which effects of equivalence ratio of hydrogen/air mixtures on impulse-bit are plotted. From the figure, it can be seen that the impulse-bit rapidly increases with equivalence ratios of $\phi = 0.8$ to 1.2 and then gradually decreases, showing peak values at $\phi = 1.2$ for each case. The peak values for spark ignition and laser ignition are 0.14 mNsec and 0.23 mNsec, respectively.

From these results, it is shown that higher impulse-bits can be obtained with laser ignition. Since a peak power of the laser pulse in this experiment is high enough to induce an initial blast wave at the focal point initiating a strong reacting wave, a higher impulse can be generated more effectively than the conventional spark ignitions.

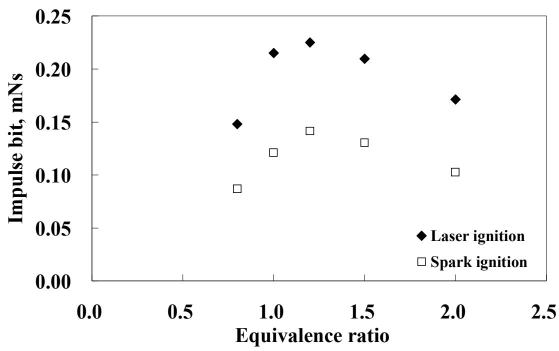

Figure 10. Impulse-bit (ignition energy 175mJ)

4.2. Effect of Orifice Size on Thrust Performance

Comparison of thrust performances among different orifice sizes, i.e., ϕ4mm, 6 mm and 10 mm, is shown in Fig.11, in which effects of equivalence ratio of hydrogen/air mixtures on impulse-bit are also plotted. From the figure, it can be seen that the impulse-bit rapidly increases with equivalence ratios of $\phi = 0.8$ to 1.2 and then gradually decreases, showing peak values at ϕ = 1.2 for each case. The peak values for 10mm-orifice, 6mm-orifice and 4mm-orifice are 0.79 mNsec, 0.92 mNsec and 1.03 mNs respectively.

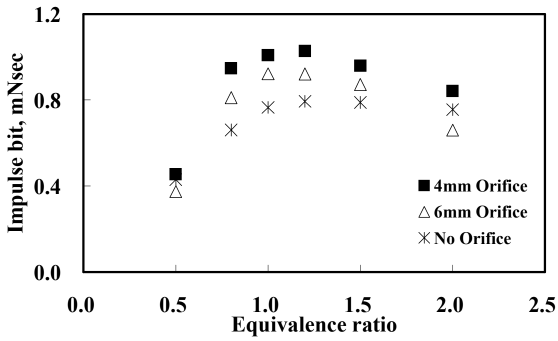

Figure 11. Impulse-bit (Orifice).

From the result, it is shown that higher impulse bit can be obtained with smaller orifices. It is also shown that the effect of the orifice is more significant when the equivalence ratio exceeds unity.

4.3. Influence of Combustor Geometry on Thrust Performance

Comparison of thrust performances between two different combustors is shown in Fig.12, in which effects of equivalence ratio of hydrogen/air mixtures on impulse-bit are also plotted. The volume of each combustor is identical, about 3.5cc, while the inner diameter of one of them is 10 mm and another of 7mm. The peak value of impulse-bit for 7mm-combustor is 0.97 mNsec at ϕ =1.0. From the result, it is shown that significantly higher impulse bit can be obtained with the narrower-shape combustor.

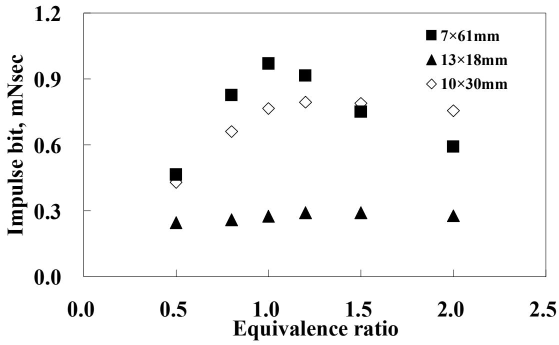

Figure 12. Impulse-bit (Different Shape).

4.4. Effect of Ignition Point.

Comparison of thrust performances among different ignition points is shown in Fig.13. In each case, the peak values appear at equivalence ratio of unity. Also, it can be seen that impulse-bits for ignition points of 10 mm and 20mm away from the closed-side of combustor are about 20 % higher than those of 0 mm and 30 mm ignition in whole equivalence ratio region. Moreover, the 10 mm case seems less sensitive to equivalence ratio.

From the result, it is confirmed that there is an optimum laser-focal position for ignition and impulse generation. Since a local equivalence ratio near the orifice can be low through the diffusion to external atmosphere, a local flame speed, when ignited at near-orifice position, may be slow causing a weak local pressure wave.

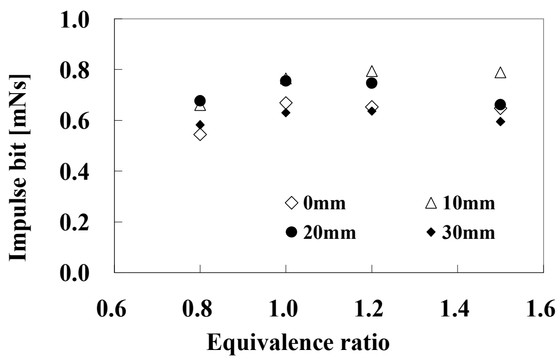

Figure 13. Impulse-bit (Ignition Point).

From these results, it is shown that even a small thruster can generate relatively high impulses when some optimum conditions are achieved. In our simulation and experimental results, the efficiency from ideal chemical energy, which is expected to be released from an ideal hydrogen-air mixture, into kinetic energy is order of a percent. There are still ways to recover this amount of loss with optimum combustor geometries and higher laser energies, and potential achieving much higher thrust performances.

5. Conclusions

A fundamental study of a laser-augmented micro-pulsejet thruster was conducted for a candidate of next-generation air-breathing micro-thruster systems. CFD analyses were conducted to evaluate internal phenomena and thrust performances for propellants of hydrogen-air mixture including effectiveness of an exhaust orifice. Experimental investigations were also conducted to evaluate effectiveness of the orifice and optimum geometries of the micro combustor. From the results, it was shown that the increase of laser energy and reduction of orifice diameter were more effective for thrust-performance improvement due to generation of higher internal pressure with longer duration. Moreover, it was shown that narrower configuration of the combustor was also effective. In our simulation and experimental results, the efficiency from ideal chemical energy, which is expected to be released from an ideal hydrogen-air mixture, into kinetic energy is order of a percent. There are still ways to recover this amount of loss with optimum combustor geometries and higher laser energies, and potential achieving much higher thrust performances.

References

[1]A. N. Pirri, M. J. Monsler, and P. E. Nebolsine, “Propulsion by Absorption of Laser Radiation”, AIAA. J, 12, 9, 1974
[2]K. Komurasaki, , *Proc. 46th Symposium on Space Science and Technology*, 1439-1444 (2002).
[3]H. Katsurayama and Y. Arakawa, *J. Japan Soc. Aeronautical and Space Sci.*, 53, 47-50 (2005).
[4]H. Katsurayama and Y. Arakawa, *Applied Plasma Science*, 12, 17-22 (2004).
[5]T. Miyasaka and T. Fujiwara, *Beamed Energy Propulsion (AIP Conference Proceedings Vol.702)*, 80-91 (2004).
[6]H. Shiraishi and T. Fujiwara, *J. Japan Soc. Aeronautical and Space Sci.*, 46, 607-613 (1998).
[7]T. Fukui and T. Fujiwara, *J. Japan Soc. Aeronautical and Space Sci.*, 43, 619-625 (1995).
[8]D. V. Ritzel and K. Matthews, Proc. of 21st Internal Symposium on Shock Waves, 97-102 (1997)